Investigating nonlinear dynamics from time series: The influence of symmetries and the choice of observables

Christophe Letellier

Groupe d'Analyse Topologique et de Modélisation de Systèmes Dynamiques, Université de Rouen-CORIA UMR 6614, Av. de l'Université, BP 12, F-76801 Saint-Etienne du Rouvray Cedex, France

Luis A. Aguirre

Laboratório de Modelagem, Análise e Controle de Sistemas Não Lineares, Departamento de Engenharia Eletrônica, Universidade Federeal de Minas Gerais, Av. Antônio Carlos 6627, 31270-901 Belo Horizonte, MG, Brazil

When a dynamical system is investigated from a time series, one of the most challenging problems is to obtain a model that reproduces the underlying dynamics. Many papers have been devoted to this problem but very few have considered the influence of symmetries in the original system and the choice of the observable. Indeed, it is well known that there are usually some variables that provide a better representation of the underlying dynamics and, consequently, a global model can be obtained with less difficulties starting from such variables. This is connected to the problem of observing the dynamical system from a single time series. The roots of the nonequivalence between the dynamical variables will be investigated in a more systematic way using previously defined observability indices. It turns out that there are two important ingredients which are the complexity of the coupling between the dynamical variables and the symmetry properties of the original system. As will be mentioned, symmetries and the choice of observables also has important consequences in other problems such as synchronization of nonlinear oscillators. © *2002 American Institute of Physics.* [DOI: 10.1063/1.1487570]

A great number of techniques developed for studying nonlinear dynamical systems start with the embedding of a scalar time series, lying on an m-dimensional object, in an embedding space of dimension d. Several works have analyzed how large d should be in relation to m to ensure a theoretical equivalence between the embedded dynamics and that of the original system. The main results reached are valid, in general, regardless of the observable chosen. In a number of practical situations, however, as may be expected, the choice of the observable does matter for our ability to extract dynamical information from the embedded attractor. This paper is devoted to analyzing such a problem using benchmark models. It turns out that there are two important ingredients: the complexity of the coupling between the dynamical variables, and the symmetry properties of the original system. To quantify the coupling complexity, we estimate observability indices for our examples. The ideas discussed in the paper have direct bearing on standard problems in nonlinear dynamics such as model building and synchronization.

I. INTRODUCTION

One way of investigating nonlinear behavior is by embedding a time series (as a result of the observation of the time evolution of the system) in phase space. A point in such a space is then associated with a single state of the system which is fully defined by a set of m dynamical variables. When an experimental dynamical system is investigated, these m physical quantities should be all measured, at least in

principle, to have a complete description of the state of the system under study. Unfortunately, in most experimental situations, only a single physical quantity is measured. Hence, the time evolution of the system is known through a scalar time series. The next step is therefore to reconstruct a phase space from this scalar time series. The trajectory reconstructed is thus expected to have the same properties than the trajectory embedded in the original phase space.

A pioneering paper by Packard *et al.*[1] points out two ways of reconstructing a phase space, namely, by using time delay or time derivative coordinates. Another kind of coordinates, namely principal components,[2] may also be used. Gibson *et al.*[3] demonstrated that the relationships between delays, derivatives and principal components consist of rotation and rescaling. Consequently, from Gibson's point of view, statements about the nature of the equivalence between the original and the reconstructed phase portraits would not depend on the coordinate system.

Once a phase portrait is reconstructed, it is sometimes desirable to obtain a model able to reproduce the trajectory in the reconstructed phase space (see, for instance, Refs. 4 or 5, and references therein). It may be also attempted to control the dynamical behavior using a feedback term[6,7] or to synchronize two systems.[8] In all these cases, ease of success clearly depends on the choice of observable, but this has rarely been related to the observability of the dynamics. Here we examine two aspects of this relevance for the choice of the observable: (i) the complexity of the couplings between the dynamical variables and (ii) symmetry properties. These two points of view are investigated with the aid of observ-

     1

C. Letellier and L. A. Aguirre

ability indices introduced in Refs. 9 and 10. In this paper we refine the original definition of such indices, explore aspects relating to time averaging and ergodicity.[11]

The paper is organized as follows: In Sec. II, we first present a detailed case of how the choice of observable can affect the ability to reconstruct dynamics from scalar time series. In the second part of Sec. II, the definition of an observability index is reviewed. In Sec. III, using several bench models and the observability indices we show that the nonequivalence between observables has two basically different sources, namely, (i) the couplings between the different dynamical variables, this information is quantified by the observability indices, and (ii) the presence of symmetries to which the observability indices are basically insensitive. The main conclusions of the paper are summarized in Sec. IV.

II. NONEQUIVALENCE OF THE DYNAMICAL VARIABLES: A FIRST EXAMPLE

Assume that the dynamical system under study is $\dot{x}(t) = f(x(t))$, where t is the time, $x \in \mathbb{R}^m$ is the state vector, and f is the nonlinear vector field. As often happens in experimental settings, a single physical quantity is expected to be measured. Hence, the recorded variable (also called the observable) is obtained using a measurement function $h: \mathbb{R}^m \to \mathbb{R}$ such that the recorded scalar time series $\{s(t)\}_{t=0}^t$ is given by $s(t) = h(x(t))$. This measurement function acts therefore as a projection of an m-dimensional object onto a one-dimensional space. An equivalent phase portrait is thus reconstructed using the derivative coordinates as suggested by Packard $et\ al.$[1] In this paper, most of examples will concern three-dimensional systems ($m = 3$) which will be reconstructed in a three-dimensional space. Consequently, the reconstructed portrait is spanned by the derivative coordinates acording to

$$\varphi = \begin{cases} X = s, \\ Y = \dot{s}, \\ Z = \ddot{s}. \end{cases} \tag{1}$$

A coordinate transformation Φ between the original dynamical variables (x, y, z) and the derivative coordinates (X, Y, Z) can therefore be defined. In the case where $s = x$, the transformation Φ reads

$$X = s, \quad Y = f_s, \quad Z = \frac{\partial f_s}{\partial x} f_x + \frac{\partial f_s}{\partial y} f_y + \frac{\partial f_s}{\partial z} f_z, \tag{2}$$

where f_x, f_y, and f_z are the components of f. When the derivative coordinates are used, a differential model may be written under the form,

$$\dot{X} = Y, \quad \dot{Y} = Z, \quad \dot{Z} = F_s(X, Y, Z), \tag{3}$$

where $F_s(X, Y, Z)$ is the model function.[12] Here is the great advantage of the continuous model built on the derivative coordinates because, when the original system is known, the model function F_s may be analytically derived using the coordinate transformation Φ.[10] The function F_s contains information on the nature of the coupling between dynamical variables ''seen from one observable point of view.'' Our main objective is thus to investigate how the nature of the

couplings may effect the observability of a system when the analysis is carried out from a single variable.

Let us start with a simple example. We assume that the original system is the Rössler system,[13]

$$\dot{x} = -y - z, \quad \dot{y} = x + ay, \quad \dot{z} = b + z(x - c), \tag{4}$$

where (a, b, c) are the bifurcation parameters. The cases where each dynamical variable is successively the observable are now investigated.

Let us start with the measurement function such that $s = h(x, y, z) = y$. The coordinate transformation Φ_y reads then as

$$\Phi_y = \begin{cases} X = y, \\ Y = x + ay, \\ Z = -y - z + ax + a^2 y, \end{cases} \tag{5}$$

and the corresponding model function F_y is

$$F_y = -b - cX + (ac - 1)Y + (a - c)Z - aX^2$$
$$+ (a^2 + 1)XY - aXZ - aY^2 + YZ. \tag{6}$$

This is a very favorable case because the determinant of the Jacobian matrix $\mathcal{J}(\Phi_y)$ never vanishes and it may be easily shown that Φ_y is injective. The coordinate transformation Φ_y therefore defines a diffeomorphism from the original phase space to the reconstructed one. Consequently, the Rössler system is most observable from the y-observable, i.e., the y-variable is the best observable for investigating this system from a scalar time series.

When the observable is the x variable of the Rössler system, i.e., $s = h(x, y, z) = x$, the coordinate transformation Φ_x reads as

$$\Phi_x = \begin{cases} X = x, \\ Y = -y - z, \\ Z = -x - ay - b - z(x - c), \end{cases} \tag{7}$$

and the corresponding model function F_x is

$$F_x = ab - cX + X^2 - aXY + XZ + acY + (a - c)Z$$
$$- \frac{(a + c + Z - aY + b)Y}{a + c - X}. \tag{8}$$

This function F_x is rational, i.e.; it presents a singularity at $X = a + c$ which is induced by the inverse function Φ_x^{-1}. In fact, Φ_x is injective but the determinant of its Jacobian matrix $\mathcal{J}(\Phi_x)$ vanishes for $x = a + c$. A singularity is therefore involved in this coordinate transformation. The set of points associated with the plane $x = a + c$ cannot be observed from the (X, Y, Z)-space through the x variable. Although this set is of Lebesgue measure zero, it effects the observability of the system but not too much because the singular plane is located near the outer boundary of the attractor.

The last case is to consider the z variable of the Rössler system as the observable, i.e., $s = h(x, y, z) = z$. The coordinate transformation Φ_z reads as

$$\Phi_z = \begin{cases} X = z, \\ Y = b + z(x - c), \\ Z = [b + z(x - c)](x - c) + z(-y - z), \end{cases} \tag{9}$$
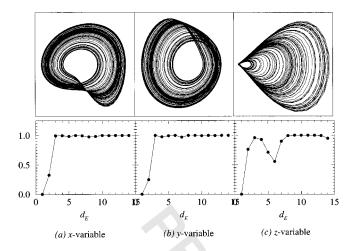
FIG. 1. The three induced phase portraits from the dynamical variables of the Rössler system using the derivative coordinates and the estimations of their embedding dimension by using the false nearest neighboor methods. $(a,b,c)=(0.398,2.0,4.0)$. The embedding dimensions are computed using delay coordinates from a time series recorded with a sampling rate equal to 0.01 s.

and the associated model function is

$$F_z = b - cX - Y + aZ + aX^2 - XY$$
$$+ \frac{(ab+3Z)Y - aY^2 - bZ}{X} + \frac{2bY^2 - 2Y^3}{X^2}. \qquad (10)$$

The complexity of the model function has increased compared to the one of the model function F_x. In this paper, complexity designates the number of monomials involved in the model function as well as the order of the nonlinearities and of the poles. Thus, a model function with a large number of monomials with high order of nonlinearities or, in a stronger way, with high order for the poles, is more complex than a model function with few monomials with low order nonlinearities. Note that the model function expresses the couplings between the dynamical variables of the original system ''seen from one observable point of view.'' In the present case, the denominator is now a second-order polynomial. In this case, the double singularity is close to the attractor and effects the shape of its manifold. This creates a region of the z-induced attractor where different revolutions are not well distinguished [Fig. 1(c)]. Such a feature will obviously induce some difficulties in investigating the dynamics from the z-variable. Significant differences between the attractor reconstructed from the z-variable and the other two (x and y-variables) can be easily appreciated from Fig. 1.

Note that the coordinate transformation Φ_z is again injective but the determinant of its Jacobian matrix $\mathcal{J}(\Phi_z)$ vanishes when $z^2 = 0$. This is again a plane in the original phase space but its influence on the z induced attractor is more important since it is an order-2 singularity. On the other hand, the couplings between the dynamical variables are more complicated when they are observed from the z variable. The nonequivalence among the dynamical variables is confirmed when the embedding dimension is computed. For the x and y-induced phase portraits, such a dimension is

clearly equal to 3 but it is much more difficult to state about the embedding dimension of the z induced phase portrait (Fig. 1).

The observability of the dynamics from a scalar time series appears to be related to the complexity of the model function and the presence of singular sets. Based on the complexity of Φ_x, Φ_y, and Φ_z the dynamical variables may be classified as $y \triangleright x \triangleright z$, where $\triangleright$ means ''provides a better observability of the underlying dynamics than.'' It should be noted that when a global model is attempted using a global modeling technique, the y variable allows to obtain a global model with relative ease while the z-variable provides a very difficult test case and so far no three-dimensional global models have been obtained unless an ad hoc structure is used.[10,11] The previous order is therefore strongly related to the difficulty to obtain a global model from a scalar time series.

For the Rössler system, which has no symmetry, the observability indices convey significant information. We saw that the y turns out to be the best variable while, on the other hand z, is by far the worst. This can be confirmed in a number of ways, as for instance the easiness with which one can obtain a global model[10] or the possibility of synchronizing. A direct substitution synchronization scheme is only successful if the y variable is used as the driving signal.[8] Even when synchronization is attempted using adaptative control techniques the conclusion is the same, namely that no synchronization is possible driving the slave system either with the x or the z variables.[14] The possibility or easiness of synchronization will not only depend on observability but will also be effected by the way synchronization is attemped. For instance, if proportional linear negative feedback is used instead of direct substitution it is possible to synchronize two Rössler systems. However, if the variable x is used it will require greater effort to synchronize (with the same performance) than if y is used. Hence, although there seems to be some relation between observability and synchronization we cannot, now, make any generalization.[15,16]

The nonequivalence between the dynamical variables of a system can be made somewhat by quantifying the observability with an index as introduced in Refs. 9 and 10. The concept of observability in linear system theory is standard.[9,17] Consider the system,

$$\dot{x} = Ax + Bu, \quad s = Cx, \qquad (11)$$

where $x \in \mathbb{R}^n$ is the state vector, $s \in \mathbb{R}^r$ is the measurement vector, $u \in \mathbb{R}^p$ is the input vector, and $\{A,B,C\}$ are constant matrices. For a nonlinear system, A is the Jacobian matrix of that system, B is the matrix defining the coupling between the system, and an external contraint and C defines the measurement function designated by h. In all the cases here investigated, the systems are autonomous, i.e., $B = 0$ or $u = 0$. Thus the system (11) is said to be state observable at time t_f if the initial state $x(0)$ can be uniquely determined from knowledge of a finite time history of the output $y(\tau)$, $0 \leq \tau \leq t_f$,[17] since the input $u(\tau) = 0$.

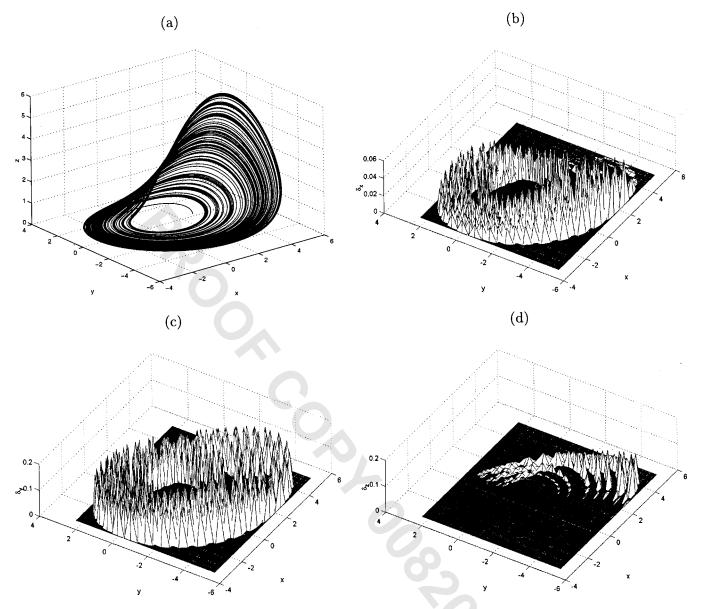One way of testing whether the system (11) is observable is to define the *observability matrix*,

(a)

(b)

(c)

(d)

FIG. 2. (a) The Rössler attractor. (b), (c), and (d) are, respectively, the local observability indices δ_x, δ_y, and δ_z projected onto the $x \times y$ plane. Higher peaks indicate higher observability. Recall that δ_x is the observability attained when observing the system only through variable $x(t)$.

$$Q = \begin{bmatrix} C \\ CA \\ CA^2 \\ \vdots \\ CA^{n-r} \end{bmatrix}. \tag{12}$$

The system (11) is therefore state observable if matrix Q is full rank, that is if rank$(Q)=n$. This definition is a ''yes'' or ''no'' measurement of observability, that is, the system is either observable or not. In practice, however, a system may gradually become unobservable as a parameter is varied or, for nonlinear systems, it seems reasonable to suppose that there are regions in phase space that are less observable than others. We quantify the degree of observability with the observability index, defined as

$$\delta(\boldsymbol{x}) = \frac{|\lambda_{\min}[QQ^T, \boldsymbol{x}(t)]|}{|\lambda_{\max}[QQ^T, \boldsymbol{x}(t)]|}, \tag{13}$$

where $\lambda_{\max}[QQ^T, \boldsymbol{x}(t)]$ indicates the maximum eigenvalue of matrix QQ^T estimated at point $\boldsymbol{x}(t)$ (likewise for $\lambda_{\min}$) and $(\cdot)^T$ indicates the transpose. Then $0 \leq \delta(\boldsymbol{x}) \leq 1$, and the lower bound is reached when the system is unobservable at point $\boldsymbol{x}$. It should be noticed that the index (13) is a type of condition number of the observability matrix. The matrix A takes into account the coupling between the original dynamical variables while the matrix C corresponds to the measurement function h. If the measurement function is defined by an identity matrix, the dynamics is completely observable. When a single variable is measured, matrix C becomes a row vector and is directly responsible for any decrease in observability.

From the definition, it becomes clear that $\delta(\boldsymbol{x})$ is a local measure, which obviously depends on the point $\boldsymbol{x}$ in state space where the system is. To see this more clearly, Fig. 2 shows the local observability indices δ_x, δ_y, and δ_z pro-

jected onto the $x \times y$ plane. Higher peaks indicate higher observability.

The following remarks can be made. When observing the system through variable $x(t)$, the least observable part of the attractor is precisely when the trajectories start to depart from the neighborhood of the $x \times y$-plane because the sheet-like vertical part of the attractor faces the y-axis and can only be seen sideways from the x-axis. This explains why the observability index δ_y does not decrease in that part of the attractor. For a similar reason, the observability from the z variable is very low in parts of the attractor that are in the neighborhood of the $x \times y$-plane, as seen in Fig. 2(d).

It is also interesting to notice that the plots in Fig. 2 are in agreement with Eqs. (5)–(10). In particular, consider the model function F_x that results when the dynamics of this system are reconstructed from the x variable only. From Eq. (8) it is clear that such a function becomes singular at $x=a+c$. The aforementioned plots were obtained for $a=0.398$, $b=2.0$, and $c=4.0$. Therefore the singular plane is $(\mathbf{x}|x=4.398)$, which agrees with the least observable region seen in Fig. 2(b). Similarly, Eq. (10) becomes singular at $z=0.0$, that is, at the $x \times y$-plane. This can be clearly seen comparing Fig. 2(a) and Fig. 2(d). Finally, funcion (6) does not become singular at any point in space thus resulting in great observability at any point on the attractor as seen in Fig. 2(c).

The observability indices illustrated in Figs. 2(a)–2(c) were calculated along a trajectory embedded in the Rössler attractor. We obtain basically the same result whether we calculate the observability indices using a single increasingly long trajectory, or an increasingly large set of trajectories starting from random initial conditions (Fig. 2). This suggests ergodicity, at least to some extent.

It will be convenient to summarize the observability attained from a given variable using an average value. In this respect, the two following possibilities should be considered:

$$\varrho = \frac{1}{T} \sum_{t=0}^{T} \delta(\mathbf{x}(t)) \tag{14}$$

and

$$\bar{\delta} = \frac{\frac{1}{T} \sum_{t=0}^{T} \lambda_{\min}[QQ^T, \mathbf{x}(t)]}{\frac{1}{T} \sum_{t=0}^{T} \lambda_{\max}[QQ^T, \mathbf{x}(t)]}, \tag{15}$$

where T is the final time considered and, without loss of generality the initial time was set to be $t=0$.

For the three dynamical variables of the Rössler system (4), the observability indices averaged in both ways are shown in Table I for comparison.

From Table I both ways of estimating the observability indices yield results which are within one standard deviation from each other. This suggests that the error is not statistically significant. However, for the sake of presentation, unlike Ref. 10, it will be preferred to use $\bar{\delta}$ rather than ϱ because this seems to be somewhat closer in spirit to the procedure followed in estimating Lyapunov exponents. Also,

TABLE I. Observability indices for the Rössler system averaged in different ways. The σ indicates the respective standard deviation.

$\delta \pm \sigma_\delta$	$\bar{\delta} \pm \sigma_\delta$
$\varrho_x = 0.025 \pm 0.014$	$\bar{\delta}_x = 0.022 \pm 0.014$
$\varrho_y = 0.133 \pm 1.7 \times 10^{-14}$	$\bar{\delta}_y = 0.133 \pm 1.7 \times 10^{-14}$
$\varrho_z = 0.010 \pm 0.024$	$\bar{\delta}_z = 1.9 \times 10^{-4} \pm 0.024$

from the values in Table I, the variables can be ranked in descending degree of observability according to

$$y \rhd x \rhd z, \tag{16}$$

which precisely agrees with the sequence found in Sec. II where the complexity of model functions Φ_i was investigated in a rather detailed way.

As a final observation on the indices, we simulated the Rössler system with the same parameter values and over the same length of time, but with one hundred random initial conditions, yielding one hundred different values of $\bar{\delta}$. Taking the ensemble average and standard deviation then gave us an idea of how sensitive the calculations are with respect to initial conditions. The ensemble averages with respective standard deviations were $E[\bar{\delta}_x] = 0.022 \pm 4.4 \times 10^{-4}$, $E[\bar{\delta}_y] = 0.133 \pm 1.1 \times 10^{-16}$, and $E[\bar{\delta}_z] = 2.0 \times 10^{-4} \pm 6.4 \times 10^{-6}$. These results show that whereas the ensemble average is very close to the time average (see Table I), that is, along the trajectory, the ensemble standard deviation is typically two orders of magnitude smaller than the counterpart take along a trajectory. Again, this suggests that the observability index is ergodic.

In what follows $\bar{\delta}$ will be calculated for several systems with diverse dynamical properties. To this end, the time average $\bar{\delta}$ will suffice. The reader should bear in mind, however, that the observability indices are local quantities and that taking the average is useful inasmuch as it portrays an overall picture but, on the other hand, plots like those in Fig. 2 could be used to give more details on how the observability varies along the attractor.

III. PROPERTIES

A. Relevance of the nature of couplings

In the previous section, we only investigated the case where the observable is one of the dynamical variables of the original system, i.e., when the C-matrix corresponding to the measurement function has a single diagonal element equal to 1, all the others being equal to zero. This is a very particular case and, in practice, the measurement function may also be a combination of the dynamical variables. For instance, let us assume that the Rössler system is now rewritten in the phase space spanned by the coordinate sets reading as

$$x' = y+z, \quad y' = z+x, \quad z' = x+y. \tag{17}$$

The Rössler system may then be rewritten under the form,

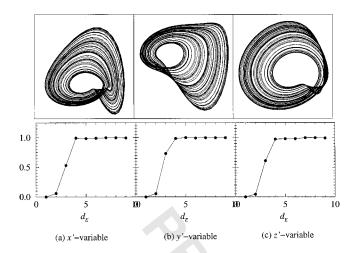$$\dot{x}' = \tfrac{1}{2}[(1-a+c)x' + (a-1+c)y' - (1+a+c)z' - 2b + \tfrac{1}{2}((x'-y')^2 - y'^2)],$$

FIG. 3. The three induced phase portraits from the rotated Rössler system using the derivative coordinates and the estimations of their embedding dimension by using the false nearest neighbors technique.

$$\dot{y}' = \frac{a}{2}[(a-1)x' + (1-a)y' + (a+1)z'] - x', \quad (18)$$

$$\dot{z}' = b - [b - \tfrac{1}{4}((x'-z')^2 + 2c(x'+y'-z') - y'^2)](c+x').$$

This system has the same fixed points than the original Rössler system and, consequently, the same manifold. But the coupling between the dynamical variables (x',y',z') are completely different than the ones between the original dynamical variables. Each dynamical variable corresponds to an observable composed of two dynamical variables of the original Rössler system according to

$$x' = s = h(\boldsymbol{x}) = y + z, \quad y' = s = h(\boldsymbol{x}) = z + x,$$
$$z' = s = h(\boldsymbol{x}) = x + y. \quad (19)$$

This coordinate transformation corresponds to a rotation of the attractor in the phase space. For the sake of simplicity, we will continue the analysis using the dynamical variables (x,y,z) of the original Rössler system. For instance, when the observable is the variable x', the coordinate transformation $\Phi_{x'=y+z}$ reads as

$$\Phi_{x'} = \begin{cases} X = y + z, \\ Y = b + x + ay - cz + xz, \\ Z = -bc + (a+b)x + (a^2-1)y + (c^2-1)z \\ \qquad - (2c+1)xz - z^2 + x^2 z. \end{cases}$$
$$(20)$$

The determinant of its Jacobian matrix vanishes for a quite complicated function depending on the system parameters. This condition defines a singularity of order-3. Moreover, the coordinate transformation $\Phi_{x'}$ cannot be inverted in the general case and, when the numerical values of the bifurcation parameters are used, the expression of $\Phi_{x'}^{-1}$ is too complicated to be useful. The observability of the dynamics from this variable would be very poor. A plane projection of the x'-induced phase portrait is displayed in Fig. 3(a). The embedding dimension is clearly equal to 4 for each of the dynamical variables (x',y',z'). From the embedding dimen-

sion point of view, all these variables are equivalent. Nevertheless, when they are compared to the original variables (x,y,z) of the Rössler system, the embedding dimension has increased, meaning that the differential embedding needs an additional dimension to unfold the attractor without any ambiguity. Hence it seems reasonable to suggest that the dynamics look more intricated in the new space.

When the y'-variable is taken as an observable, the coordinate transformation reads as

$$\Phi_{y'} = \begin{cases} X = x + z, \\ Y = -y - z + b + z(x-c), \\ Z = -b(c+1) + (b-1)x - ay + c(c+1)z \\ \qquad + (1-2c)xz - yz - z^2. \end{cases}$$
$$(21)$$

It has a Jacobian vanishing for

$$y = 1 + (1+c)a - b + c(c+1) - x(1+2c+a)$$
$$+ (3c+a)z + x^2 - 3xz + z^2 \quad (22)$$

which defines a singularity of order-1.

Finally, when the z'-variable is the observable, the coordinate transformation $\Phi_{z'}$

$$\Phi_{z'} = \begin{cases} X = x + y, \\ Y = x + (a-1)y - z, \\ Z = -b + (a-1)x + (a^2-a-1)y \\ \qquad + (c-1)z - xz, \end{cases}$$
$$(23)$$

has a Jacobian vanishing for

$$z = (2c + 3a - ac - a^2 - 2) + (a-2)x, \quad (24)$$

which defines a singularity of order-1. The most interesting property of these observables is that the model functions $F_{y'}$ and $F_{z'}$ are polynomial. Although there are monomials that include non integer power of the derivatives, there is no pole involved and such a function would be less difficult to estimate from data set than for rational functions. Let us note that the model function $F_{y'}$ is much more complicated (a larger number of terms) than the model function $F_{z'}$.

This analysis in terms of the complexity of dynamical couplings suggests the observability order $z' \rhd y' \rhd x'$. Again, this analysis is confirmed by the observability indices which are

$$\delta_{x'} = 0.005, \quad \delta_{y'} = 0.010, \quad \delta_{z'} = 0.044. \quad (25)$$

The indices are effected by this rotation of the attractor in the phase space although the topology is preserved. What is modified is in fact the couplings between the dynamical variables used for describing the attractor. The couplings are therefore relevant for the nonequivalence between the dynamical variables since only a rigid displacement of the attractor has been applied, i.e., the dynamics is not changed at all. Thus, for a given invariant set, the observability of a given dynamical system depends crucially on the choice of the observable.

B. Effects of symmetries

Another important point is to investigate how the symmetry properties may effect the observability of a dynamical system when viewed from a single time series. Indeed, when

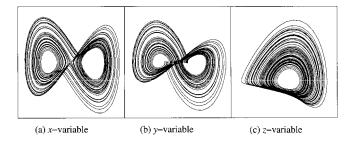(a) x–variable　　　　(b) y–variable　　　　(c) z–variable

FIG. 4. The three induced phase portraits of the Lorenz system. While the x and y-induced attractors have an inversion symmetry, the z one does not have any symmetry.

the system under study presents some symmetry properties, particular features may appear. A system possessing some kind of symmetry is said to be equivariant, i.e., there is an operator Γ such that

$$\Gamma \cdot f(x) = f(\Gamma \cdot x), \tag{26}$$

where Γ is a square $m \times m$ matrix defining the symmetry. For instance, the Lorenz system[18] is equivariant. The dynamical system equations read as

$$\dot{x} = \sigma(y-x), \quad \dot{y} = Rx - y - xz, \quad \dot{z} = -bz + xy, \tag{27}$$

where σ is the Prandtl number, R is the reduced Rayleigh number, and b is an aspect ratio of the convection cell. When the bifurcation parameter values are set to 10.0, 28.0, and 8/3, respectively, the asymptotic behavior settles down onto a chaotic attractor which is setwise symmetric under a rotation around the z-axis. In such a case, the operator Γ reads as

$$\Gamma = \begin{bmatrix} -1 & 0 & 0 \\ 0 & -1 & 0 \\ 0 & 0 & 1 \end{bmatrix}, \tag{28}$$

that is, the chaotic attractor is globally invariant under the map $(x,y,z) \rightarrow (-x,-y,z)$. Two kinds of dynamical variables may be distinguished. First, the x and y variables are mapped to their counterpart under the action of the symmetry. As a consequence these variables allow to distinguish the two wings of the attractor. Second, the z-variable is unchanged under the action of the symmetry. This variable does not therefore provide any information about the symmetry of the attractor, i.e., the two wings are not distinguished (Fig. 4).[19]

However, the observability indices for this system,

$$\bar{\delta}_x = 6.5 \times 10^{-6}, \quad \bar{\delta}_y = 8.2 \times 10^{-6}, \quad \bar{\delta}_z = 2.2 \times 10^{-5}, \tag{29}$$

would seem to suggest the observability order $z \triangleright y \triangleright x$. For the Lorenz system a new ingredient plays an important and fundamental role, namely, the rotation symmetry. In this case, as argued, the observability indices, as a consequence of being a local quantity averaged over the attractor, does not convey all the information required for a more precise analysis. Indeed, the symmetry properties can only be identified at a global point of view, an equivariant dynamics and its image without any residual symmetry being locally equivalent.[20] As a matter of fact, because observations of the z-variable actu-

ally mod out the symmetry, it is rather impossible to recover such a symmetry from a global model obtained through the z variable. It should be noted however that, disregarding the fact that such models cannot possibly display a symmetry which cannot be observed, quite accurate global models from the the z variable can be obtained quite easily[4] (as suggested by the high observability index). The moding out of the rotation symmetry is also quite restrictive from the point of view of master-slave systems, in which case it is well known that synchronization fails in a number of different approaches when the z-variable is transmitted.[8,14]

We have now to check whether the increase in observability arises from the modding out of symmetries or from the lower complexity of couplings. We will therefore consider the case of an equivariant system and its image system.[20] An image system is a system which is dynamically equivalent to an equivariant system but without any symmetry properties. The Lorenz system and its image, the so-called proto-Lorenz introduced by Miranda and Stone[21] will be analyzed.

The image of the Lorenz system may be derived by modding out the symmetry with the aid of the coordinate transformation;

$$\Psi = \begin{cases} u = x^2 - y^2, \\ v = 2xy, \\ w = z \end{cases} \tag{30}$$

as introduced by Miranda and Stone.[21] Such a map is typical for rotation symmetry by π around the z-axis. The image system thus reads as

$$\dot{u} = (-\sigma - 1)u + (\sigma - R)v + vw + (1-\sigma)\rho,$$

$$\dot{v} = (R-\sigma)u - (\sigma+1)v - uw + (R+\sigma)\rho - \rho w, \tag{31}$$

$$\dot{w} = -bw + \tfrac{1}{2}v,$$

where $\rho = \sqrt{u^2 + v^2}$. It may be easily checked that the attractor solution of the image system is topologically equivalent to the z-induced attractor of the Lorenz system (Fig. 5).

The overall dynamics of the image system is clearly simpler than the original Lorenz system because the former does not have any symmetries. On the other hand, as can be easily verified comparing Eqs. (27) and (31), the couplings between the dynamical variables (u,v,w) are somewhat more complicated than the couplings among the original dynamical variables (x,y,z) of the Lorenz system. Such an additional complexity of the dynamical couplings in the image system is accompanied by an expected decrease of the observability indices, which for system (31) are

$$\bar{\delta}_u = 1.44 \times 10^{-8}, \quad \bar{\delta}_v = 1.60 \times 10^{-7}, \quad \bar{\delta}_w = 3.76 \times 10^{-7}. \tag{32}$$

From the stand point of symmetries, the image system is, of course, more observable than the original Lorenz system, because when such a system is observed from the w-variable no symmetry is modded out and there is no ambiguity as to where the system is in phase space. This confirms that the observability indices do not convey information about the system symmetry.
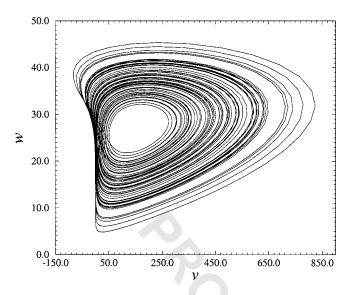
FIG. 5. The proto-Lorenz system represents an image of the Lorenz system, i.e., a system with equivalent dynamics but without any symmetry properties.

To notice that the time evolutions of the z-variable of the Lorenz system and of the w-variable of the image system are rigorously identical and, consequently, they provide the same induced phase portrait spanned by their derivatives. Thus, the observability indices strongly depend on the couplings between the dynamical variables, as argued in Sec. II. It should be mentioned that we do not usually compare the observability indices among systems because they do not seem to have an "absolute" significance. However, an image system is here compared with its twofold cover, i.e., the proto-Lorenz system with the Lorenz system. In that case, the dynamics is equivalent modulo the symmetry properties. Only the symmetries induce different couplings between the dynamical variables.

As a final example, we will focus our attention on a 5D dynamical system which presents a continuous rotation symmetry. The set of Eqs. (33), shown below, describes a laser system for which the detuning δ between the normalized steady-state laser frequency and the molecular resonnance frequency is taken into account.[22] It reads as

$$\dot{x}_1 = -\sigma(x_1 + \delta x_2 - y_1), \quad \dot{x}_2 = -\sigma(x_2 - \delta x_1 - y_2),$$

$$\dot{y}_1 = R x_1 - y_1 + \delta y_2 - x_1 z, \tag{33}$$

$$\dot{y}_2 = R x_2 - \delta y_1 - y_2 - x_2 z, \quad \dot{z} = -\gamma z + x_1 y_1 + x_2 y_2,$$

where R is the pumping rate, σ is the ratio of the cavity decay rate of the field in the cavity over the relaxation constant of the polarization, and γ is the relaxation constant of the normalized inversion. (x_1, x_2) are the real and imaginary parts of the electric field, (y_1, y_2) are real and imaginary parts of the amplitude of polarization, and z is the normalized inversion.[22] The system (33) has one fixed point F_0 located at the origin of the phase space and a continuous set of fixed points where

$$x_1^2 + x_2^2 = \gamma(R - 1 - \delta^2),$$

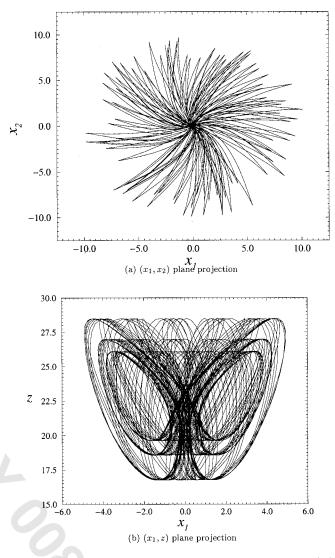$$y_1^2 + y_2^2 = (1 + \delta^2)\gamma(R - 1 - \delta^2), \quad z = R - 1 - \delta^2. \tag{34}$$

(a) (x_1, x_2) plane projection

(b) (x_1, z) plane projection

FIG. 6. Plane projections of the attractor solution of the laser system (33) ($R = 24.0$, $\sigma = 2.0$, $\gamma = 0.25$, and $\delta = 0.1$). The angular velocity depends linearly on the detuning δ.

This set of fixed points is in fact a torus T^2. It should be noticed that the z-variable is unchanged under the action of the rotation symmetry which acts independently on the (x_1, x_2) and (y_1, y_2) planes.[23] The effect of the continuous rotation is displayed in Fig. 6 for $\delta = 0.60$.

Figure 7 shows the embedding dimension estimated from each state variable. For x_1, x_2, y_1, and y_2, which are changed under the action of the symmetry, the embedding dimension is around 5 or 6, whereas the phase portrait induced by the z-variable, which is invariant under the action of the symmetry, is characterized by an embedding dimension equal to 3 (Fig. 7). This means that the whole set of dynamical variables is, in principle, observable from the variables x_1, x_2, y_1, and y_2 while only three dimensions can be distinguished when observing the dynamics from the z-variable. Indeed, when the dynamics is investigated from the z-variable, the symmetry properties are modded out (Fig. 8) as well as the distinction between the x_1 and x_2 variables, and, y_1 and y_2. Thus, two dimensions are roughly unobservable.
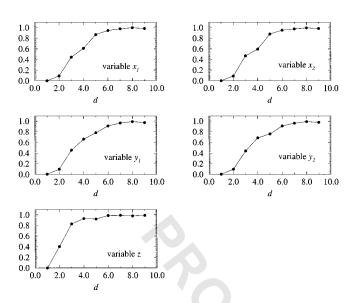
FIG. 7. Estimation of the embedding dimension using a false nearest neighbors technique for the phase portraits induced by the different dynamical variables ($R=24.0$, $\sigma=2.0$, $\gamma=0.25$, and $\delta=0.1$).

In fact the embedding dimension equal to 3 for the z-induced phase portrait may be theoretically justified when the rotation vanishes, that is, when the detuning, δ, is set to zero. In that case, the 5D laser system (33) is reduced to

$$\dot{x}_1 = -\sigma(x_1-y_1), \quad \dot{x}_2 = -\sigma(x_2-y_2),$$
$$\dot{y}_1 = -y_1+Rx_1-x_1z, \quad \dot{y}_2 = -y_2+Rx_2-x_2z, \quad (35)$$
$$\dot{z} = -\gamma z+x_1y_1+x_2y_2.$$

The variables x_1 and x_2 (resp. y_1 and y_2) become identical and the system is reduced to a slightly modified 3D Lorenz system,

$$\dot{x} = -\sigma(x-y), \quad \dot{y} = -y+Rx-xz, \quad \dot{z} = -\gamma z+2xy. \quad (36)$$
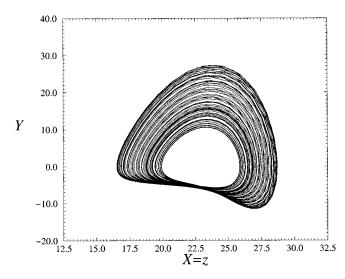
The observability indices

FIG. 8. Plane projection of the z-induced phase portrait spanned by the derivative coordinates. The same bifurcation parameters than for Fig. 7 are used. The z-induced phase portrait (Fig. 8) which is very similar to the image of the 3D Lorenz system (Ref. 23).

$$\bar{\delta}_{x_1} = 5.19\times10^{-7}, \quad \bar{\delta}_{x_2} = 5.79\times10^{-7},$$

$$(37)$$

$$\bar{\delta}_{y_1} = 1.94\times10^{-7}, \quad \bar{\delta}_{y_2} = 2.31\times10^{-7}, \quad \bar{\delta}_z = 4.52\times10^{-9}$$

seem to confirm the fact that the dynamics is less observable from the z-variable than from the other variables. An important remark should be given here. It is definitely easier to investigate the laser dynamics from the z-variable, that is when the symmetries are modded out,[19] but in this particular case, it is not associated with the greater observability index because two variables are also modded out as clearly exhibited by the estimation of the embedding dimension, which, due to the symmetry, is less than the dimension of the original phase space.

This example brings out the important fact that observability and embedding dimension are two different things which are not always correlated. This is also the first example where the embedding dimension is less than the dimension of the original phase space. This example shows also that a symmetry of the original phase portrait may induce some lack of observability when a particular observable is used. For instance, information on detuning cannot be recovered from the z-observable. In our experience, systems with inversion symmetry are harder complicated to investigate than those with an order-2 rotation. In particular, in the case of a system with an inversion symmetry, the image without any residual symmetry has often an entangled manifold. This is due to the strong singularity located at the origin of the phase space. Moreover, we believe that higher the symmetry order, the less observable the dynamics.

We see from this analysis that our ability to investigate an equivariant dynamical system depends on the couplings between the dynamical variables *and* the symmetry properties. Indeed, the observability indices do not convey much information on symmetry, since they are defined as average of local quantities along the trajectory. For instance, in the Lorenz system, it is not possible to determine on which wing the trajectory is when the z-variable is the observable. No information on the symmetry of the system is thus available. This is not a great problem when a no-symmetry global model is attempted. The obtained model reproduces the dynamics of the image system and in such a case only the complexity of couplings are relevant. Contrary to this, when synchronization of two Lorenz systems is attempted using the z-variable as the drive, it is not possible to reach a synchronization state.[8,14] Such a feature may be explained on the symmetry properties of the system and not with the observability indices.

IV. CONCLUSION

This paper has investigated the nonequivalence between the variables of nonlinear systems for observing the underlying dynamics. We have shown that this is easier using some variables than with others, and quantified the easiness with observability indices. The observability indices do not convey much information on symmetry as a consequence of being defined as averages of local measures along a trajectory. The analysis systems with symmetry may need a global

measure of observability, or perhaps the spatial distribution of local observabilities. The observability indices quantify how much the couplings between the variables departs from the linearity, as seen through a given observable. They do not depend on the topology of the attractor but rather on the orientation of the attractor in the phase space. A complete analysis, however, must take into account not only the observability indices but also the symmetry properties. When the system does not present any symmetries the observability indices convey much information.

In order to compute the observability indices the system Jacobian is used and assumed known. Consequently, at the moment, such indices seem to be well-suited for theoretical analysis of known systems rather than a practical tool to help select observables in a practical set-up. The nonequivalence between the dynamical variables of a given system may explain many results observed in the litterature. Indeed, it is now known that the success of obtaining global models depend crucially on the variable chosen as the observable. Such results may also help choose variables for synchronization.

ACKNOWLEDGMENTS

[1] N. H. Packard, J. P. Crutchfield, J. D. Farmer, and R. S. Shaw, "Geometry from a time series," Phys. Rev. Lett. **45**, 712–716 (1980).

[2] D. S. Broomhead and G. P. King, "Extracting qualitative dynamics from experimental data," Physica D **20**, 217–236 (1986).

[3] J. F. Gibson, J. D. Farmer, M. Casdagli, and S. Eubank, "An analytic approach to practical state space reconstruction," Physica D **57**, 1–30 (1992).

[4] G. Gouesbet and C. Letellier, "Global vector field reconstruction by using a multivariate polynomial L_2-approximation on nets," Phys. Rev. E **49**, 4955–4972 (1994).

[5] L. A. Aguirre and S. A. Billings, "Retrieving dynamical invariants from chaotic data using NARMAX models," Int. J. Bifurcation Chaos Appl. Sci. Eng. **5**, 449–474 (1994).

[6] E. Ott, C. Grebogi, and J. A. Yorke, "Controlling chaos," Phys. Rev. Lett. **64**, 1196–1199 (1990).

[7] K. Pyragas, "Continuous control of chaos by self-controlling feedback," Phys. Lett. A **170**, 421–428 (1990).

[8] L. M. Pecora and T. L. Carroll, "Synchronization in chaotic systems," Phys. Rev. Lett. **64**, 821–824 (1990).

[9] L. A. Aguirre, "Controllability and observability of linear systems: Some noninvariant aspects," IEEE Trans. Educ. **38**, 33–39 (1995).

[10] C. Letellier, J. Maquet, L. Le Sceller, G. Gouesbet, and L. A. Aguirre, "On the nonequivalence of observables in phase space reconstructions from recorded time series," J. Phys. A **31**, 7913–7927 (1998).

[11] L. Le Sceller, C. Letellier, and G. Gouesbet, "Structure selection for global vector field reconstruction by using the identification of fixed points," Phys. Rev. E **60**, 1600–1606 (1999).

[12] G. Gouesbet and J. Maquet, "Construction of phenomenological models from numerical scalar time series," Physica D **58**, 202–215 (1992).

[13] O. E. Rössler, "An equation for continuous chaos," Phys. Lett. A **57**, 397–398 (1976).

[14] A. Maybhate and R. E. Amritkar, "Use of synchronization and adaptive control in parameter estimation from a time series," Phys. Rev. E **59**, 284–293 (1999).

[15] H. D. I. Abarbanel and M. B. Kennel, "Local false nearest neighbors and dynamical dimensions from observed chaotic data," Phys. Rev. E **47**, 3057–3068 (1993).

[16] L. Cao, "Practical method for determining the minimum embedding dimension of a scalar time series," Physica D **110**, 43–52 (1997).

[17] T. Kailath, *Linear Systems* (Prentice–Hall, Englewood Cliffs, 1980).

[18] E. N. Lorenz, "Deterministic nonperiodic flow," J. Atmos. Sci. **20**, 130–141 (1963).

[19] C. Letellier and G. Gouesbet, "Topological characterization of reconstructed attractors modding out symmetries," J. Phys. II **6**, 1615–1638 (1996).

[20] C. Letellier and R. Gilmore, "Covering dynamical systems: Twofold covers," Phys. Rev. E **63**, 016206 (2001).

[21] R. Miranda and E. Stone, "The proto-Lorenz system," Phys. Lett. A **178**, 105–113 (1993).

[22] H. Zeghlache and P. Mandel, "Influence of detuning on the properties of laser equations," J. Opt. Soc. Am. B **2**, 18–22 (1985).

[23] C. Letellier, "Modding out a continuous rotation symmetry for disentangling a laser dynamics," *Int. J. Bifurcation Chaos* (in press).